

Brightness Discontinuities in the Northern Sub-cluster of Abell 115

K. Gutierrez,¹ H. Krawczynski,¹ and D. Harris²

¹ *Washington University in St. Louis (MO); mrgground@hbar.wustl.edu* and

² *Smithsonian Astrophysical Observatory, 60 Garden Street, Cambridge, MA 02138*

In an examination of the northern sub-cluster of A115 in a 50 ksec Chandra ACIS-I exposure we discovered several jumps in the X-ray surface brightness of the intracluster medium (ICM) in the south-western section of the sub-cluster. Examination of the surface brightness profiles reveals that these discontinuities are real and can be modeled with a central sphere and three concentric shells, each of constant emissivity. Although the dense ICM of the northern sub-cluster appears to be pushing through the thinner ICM surrounding the sub-cluster, we do not find evidence for a shock associated with any of these discontinuities. The pressure jump of 1.7×10^{-10} dyne cm^{-2} between the first and second shell (innermost and next out) is not accompanied by a corresponding temperature jump, the temperatures being roughly the same (~ 2.7 keV) within both shells. The pressure jump gives an upper limit on the velocity of the inner shell of Mach 0.589 through the outer shell. The core of the northern sub-cluster is significantly cooler (1.61 ± 0.14 keV) than the outer shells (2.59-2.89 keV). The cooling time of the core (2.95×10^8 years) is significantly shorter than the Hubble time, confirming the presence of a strong cooling flow. Finally, we discuss the correlation of the X-ray surface brightness distribution with the morphology of the radio galaxy 3C 28 at the center of the northern sub-cluster.

1. Introduction

A115 is a rich galaxy cluster (richness class 3) with two strong peaks in the X-ray surface brightness distribution (Abell et al. 1989). A115 has also been observed in the radio (Giovannini Feretti) as well as optically (Beers et al. 1983). It was resolved as a binary X-ray source by the Einstein observatory (Forman et al. 1981). Observation with the ASCA satellite (Shibata et al. 1999) indicated strong temperature variations across the cluster with the two main X-ray peaks being cooler (5 keV) than the region in between (11 keV). The double peaked X-ray surface brightness distribution and the large temperature variation between the surface brightness peaks shows that A115 is a merging system. The cluster is also interesting because it contains a strong radio galaxy 3C 28.

In this paper we present in Section 2 the data analysis and data cleaning. We present the results on the overall morphology of the binary merger in subsection 3.1. We describe the temperature structure of the northern sub-cluster in subsection 3.2, and the structure of the northern sub-cluster in subsection 3.3. Finally, we discuss the correlation of the X-ray surface brightness and the radio morphology of 3C 28 in subsection 3.4.

In the following we use $H_0 = 65 \text{ km s}^{-1} \text{ Mpc}^{-1}$ and $q_0 = 0.5$ putting the cluster at a distance of 950 Mpc; 1' corresponds to 4.6 kpc.

2. Observations and Data Preparation

We observed A115 using the ACIS I detector for 50.4 ks, on July 11, 2002. The observation used the ACIS chips I0-I3 as well as S6. The S7 chip was turned off

to keep the telemetry rate low during background flares. The data were taken in Very Faint Mode to minimize background counts. We are using the full data set as we found no background flares. We then applied a filtering process specifically designed for Very Faint Mode observations that uses a 5×5 pixel event island rather than the standard 3×3 island to distinguish between X-ray events and cosmic ray events. The filtering resulted in a 2% drop in signal and a 30% drop in background. We flat-fielded the image using exposure maps in the 0.5-1 keV, 1-2 keV, and 2-5 keV bands. We then added these images with a spectral weight to produce the final image.

The analysis was performed with the analysis package CIAO 2.3. We used an off-cluster region as background in our spectral analysis. The exact regions will be described in the results section. Only events from 0.5 keV to 6 keV were used in spectral analysis. Above 6 keV the signal-to-noise ratio is poor; below 0.5 keV the response of the instrument is plagued by systematic uncertainties. The main thrust of our analysis concentrated on the northern sub-cluster surrounding the radio galaxy 3C 28. The study of the morphological correlation between the ICM surface brightness distribution and the radio emission of 3C 28 used the 1.4 GHz radio image of 3C 28 from Feretti et al. (1984).

3. Results

3.1. Overall Morphology of the Binary Merger

The cluster A115 is a binary galaxy cluster with two pronounced sub-clusters which appear to be coalescing in an off-axis merger as shown in Fig. 1. Intriguingly, the morphology of the merger is very similar to that of

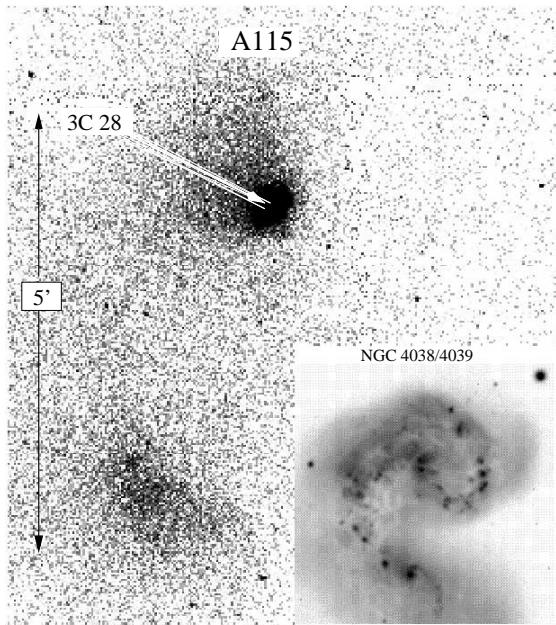


FIG. 1.— The overall structure of the galaxy cluster A115 with an inset of the Antenna galaxy (NGC 4038/4039). The similarities in structure lead us to believe that A115 is an off-axis merger with significant orbital motion of the 2 sub-clusters.

the Antenna galaxy merger as seen in the inset of Fig. 1 suggesting that tidal and MHD forces act in a similar way in both systems.

The northern sub-cluster exhibits a wedge like shape and appears to be moving in the south-west direction. The brightest region in the northern sub-cluster is centered on 3C 28.

It seems that tidal and MHD forces skewed the southern sub-cluster and resulted in a significant elongation in the north-east to south-west direction. We determined projected properties of the ICM using several regions, these regions and the background region are shown in Fig. 2.

3.2. Temperature Structure of the ICM

Using a hardness map an overall temperature structure of the cluster was determined. The coldest regions have been found at the center of the sub-clusters. The region between the two sub-clusters appears substantially hotter.

The brightest regions in both the northern and southern sub-clusters are also the coolest (2.3–3.1 keV and 3.1–3.6 keV respectively). While the cool region of the northern sub-cluster appears spherical, the cool region of the southern sub-cluster is elongated in the same direction as the X-ray source. The Chandra data confirm the presence of a hot region in between the 2 sub-clusters as reported by Shibata et al. (1999) based on ASCA observations. More detailed spectral analysis is underway.

3.3. Structure of the Northern Sub-cluster

Focusing on the northern sub-cluster we notice three brightness discontinuities. Surface brightness profiles of the southwestern section of the northern sub-cluster

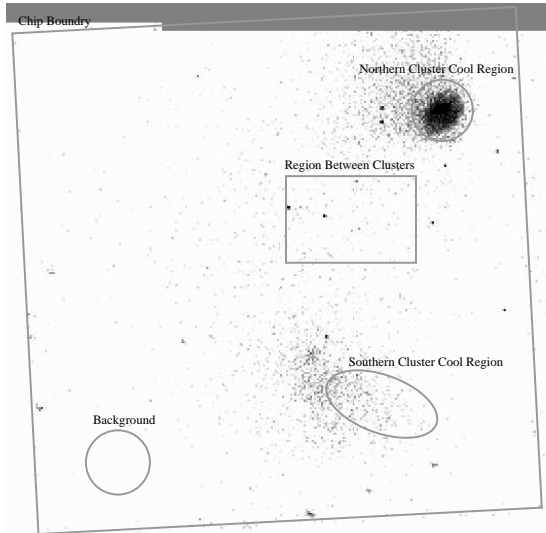


FIG. 2.— Image showing the cool regions found in both the northern and southern sub-clusters as well as the hot intermittent region. The background used in the spectral analysis is also shown.

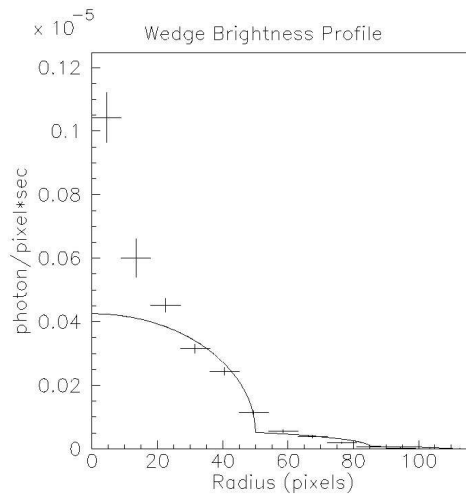


FIG. 3.— ICM surface brightness profiles of the southwestern part of the northern sub-cluster. Distance is given in instrument pixels where 1 pixel = $0''.492$. From the center to 25 pixels ($12''.3$) we see the cooling flow. From 25 to 50 pixels ($12''.3$ to $24''.6$) what we describe as the first shell. The second shell is from 50 to 85 pixels ($24''.6$ to $41''.8$). The outer shell is from 85 to 111 pixels ($41''.8$ to $54''.6$). The line shows a surface brightness model which assumes three shells of constant X-ray emissivity for the plasma in each of the three shells.

showed that these discontinuities were physical and that the ICM surface brightness is reasonably well described by a sphere surrounded by three spherical shells of constant emissivity. The discontinuities are found at a distance of $12''.3$, $24''.6$, $41''.8$ and $54''.6$ ($1'' = 3.28$ kpc) from the core of 3C 28 at the center of the northern sub-cluster. The profile of the wedge of interest (20° west of north to due south) along with the three shell model are shown in Fig. 3. At the center of the sub-cluster (within $12''.3$ of 3C 28) we see a very bright core region where the cooling flow is located. A strong brightness

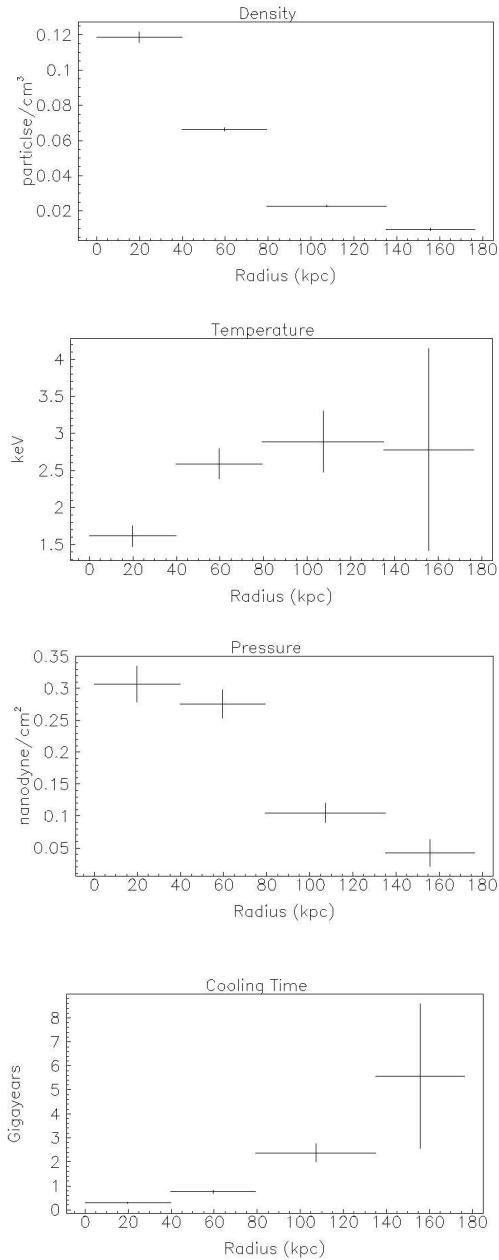


FIG. 4.— ICM particle density, temperature, pressure and cooling time profiles of the southeast part of the northern sub-cluster (20° west of north to due south of 3C 28) from the deprojection analysis with three shells and a core region.

jump is located at $24''.6$ as well as a more subtle one at $41''.8$. The first, at $24''.6$ is very strong. The second one is not highly significant. The small deviations between our model and the observed surface brightness profile indicate that the plasma emissivity is decreasing with increasing sub-cluster core distance.

We performed a deprojection analysis (Krawczynski 2002) with 4 ICM shells, the outermost shell being background. Using a single temperature Raymond-Smith plasma for each shell, we derive ICM particle density, temperature, pressure, and cooling time profiles. We show these profiles in Fig. 4.

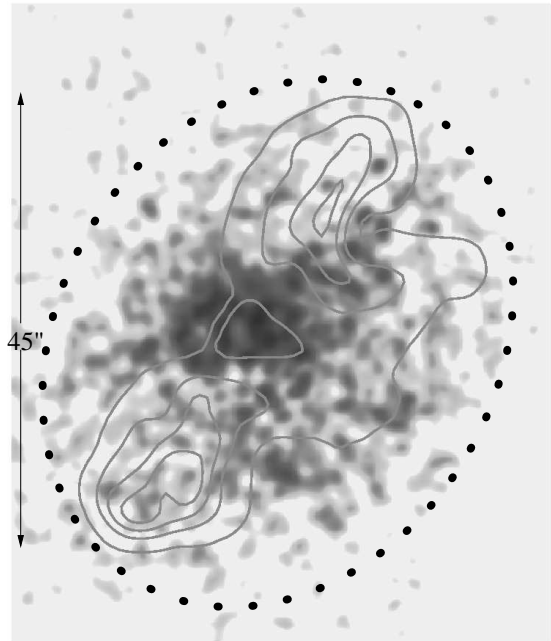


FIG. 5.— Image of the center of the northern sub-cluster. The gray-scale shows the X-ray brightness and the contours show the 1.4 GHz brightness. The X-ray bright region surrounding the radio galaxy appears to correspond to a cocoon. Also there is a correlation between the brightest triangular X-ray producing region and the radio triangle at the center of the image. The dotted ellipse shows where the brightness drops dramatically.

The first profile shows the ICM particle density. The density falls as we travel further from the center of the galaxy cluster. The resolution is not good enough to tell us if there are discontinuities between the ICM shells or whether the profile seen here is simply part of a continuous decrease of the ICM particle density. The temperature profile tell us that the temperature of the central region is cooler than the outer regions. Little detail can be obtained from the outer points on the profiles due to the large errors present. The pressure profile is the most interesting of the profiles obtained. We can see that there is a sharp pressure drop (1.7×10^{-10} dyne cm^{-2}) between the first and second ICM shells. If the pressure drop corresponds to pure ram pressure this gives us a velocity of 0.589, Mach implying that this is not a shock. The cooling time decreases as you move closer to the center of the northern sub-cluster. The fact that the cooling time in the central region is significantly smaller than the Hubble time confirms the existence of a strong cooling flow.

3.4. Correlation of X-ray Surface Brightness and the Radio Morphology of 3C 28

Focusing in to the central galaxy 3C 28, we notice in Fig. 5 a correlation between a triangular region in the center of the radio contours and surface brightness. It should also be noted that the X-ray brightness drops sharply right after the radio lobes. This may correspond to an X-ray image of the cocoon. There is no evidence found for X-ray bubbles in the image surrounding the radio lobes.

4. Discussion

The Chandra observation shows for the first time a binary merger with a very clear signature for substantial orbital movement of the two sub-clusters.

We resolved a thin X-ray producing region connecting the northern and southern sub-clusters which does not correspond to the hot region directly between the two clusters.

We find sharp brightness discontinuities. The discontinuities are somewhat similar to the sloshing central ICM regions found by Markevitch (Vikhlinin). In the case of A115 the relative movement is more pronounced compared to relaxed clusters since our cluster is in the process of merging. Indeed it looks more like a cold front found by Markevitch (Vikhlinin). In the core of the northern sub-cluster we found a correlation between the X-ray morphology and the radio morphology of 3C 28, in which the region directly surrounding the radio lobes (in a elliptical region) is bright in the X-ray.

There is a hot ICM region directly between the two X-

ray peaks. However the temperature difference we find is significantly larger than that determined by Shibata et al. (1999). We do not find a shock but we do have a dense core plunging through the ICM. The cooling time was found it to be significantly shorter than that found by Shibata et al. (1999). The latter found it to be roughly equivalent to the Hubble time. However, the estimate of Shibata et al. (1999) was based on a much larger solid angle area which covered the entire northern sub-cluster whereas we looked at the very core of the northern sub-cluster.

Acknowledgments: K. G. and H. K. downloaded the radio data from the DRAGN atlas, updated and compiled by J. P. Leahy, A. H. Bridle, and R. G. Strom. *An Atlas of DRAGNs*. K. G. and H. K. were supported by NASA/Smithsonian grant G02-3182X and D. H. was supported by NASA grant G01-2135A and NASA contract NAS 8-39073.

References

- Abell, G. O., Corwin, H. G., & Olowin, R. P. 1989, ApJS, 70, 1
 Beers, T. C., Huchra, J. P., & Geller, M. J. 1983, ApJ, 264, 356
 Feretti, L., Gioia, I. M., Giovannini, G., Gregorini, L., & Padrielli, P. 1984, A&A, 139, 50
 Forman, W., Bechtold, J., Blair, W., Giacconi, R., van Speybroeck, L., & Jones, C. 1981, ApJ, 243, L133
 Giovannini, G., Feretti, L., & Gregorini, L. 1987, A&AS, 69, 171
 Krawczynski, H. 2002, ApJ, 569, L27
 Markevitch, M., Vikhlinin, A., & Forman, W. R. 2003, in "Matter and Energy in Clusters of Galaxies," ed. S. Bowyer & C.-Y. Hwang, ASP Conf. Ser. 301, in press
 Markevitch, M. & Vikhlinin, A. 2001, ApJ, 563, 95
 Shibata, R., Honda, H., Ishida, M., Ohashi, T., & Yamashita, K. 1999, ApJ, 524, 603